

# In vitro and transdermal penetration of PHBV micro/nanoparticles

G. Eke · A. M. Kuzmina · A. V. Goreva ·  
E. I. Shishatskaya · N. Hasirci · V. Hasirci

Received: 18 June 2013 / Accepted: 27 January 2014 / Published online: 8 February 2014  
© Springer Science+Business Media New York 2014

**Abstract** The purpose of this study was to develop micro and nano sized drug carriers from poly(3-hydroxybutyrate-co-3-hydroxyvalerate) (PHBV), and study the cell and skin penetration of these particles. PHBV micro/nanospheres were prepared by o/w emulsion method and were stained with a fluorescent dye, Nile Red. The particles were fractionated by centrifugation to produce different sized populations. Topography was studied by SEM and average particle size and its distribution were determined with particle sizer. Cell viability assay (MTT) was carried out using L929 fibroblastic cell line, and particle penetration into the cells were studied. Transdermal permeation of PHBV micro/nanospheres and tissue reaction were studied using a BALB/c mouse model. Skin response was evaluated histologically and amount of PHBV in skin was determined by gas chromatography-mass spectrometry. The average diameters of

the PHBV micro/nanosphere batches were found to be 1.9  $\mu\text{m}$ , 426 and 166 nm. Polydispersity indices showed that the size distribution of micro sized particles was broader than the smaller ones. In vitro studies showed that the cells had a normal growth trend. MTT showed no signs of particle toxicity. The 426 and 166 nm sized PHBV spheres were seen to penetrate the cell membrane. The histological sections revealed no adverse effects. In view of this data nano and micro sized PHBV particles appeared to have potential to serve as topical and transdermal drug delivery carriers for use on aged or damaged skin or in cases of skin diseases such as psoriasis, and may even be used in gene transfer to cells.

## 1 Introduction

Transdermal drug applications are frequently used because of the effectiveness of the localized treatment, low cost,

---

G. Eke · N. Hasirci · V. Hasirci  
Department of Micro and Nanotechnology, Middle East  
Technical University, 06800 Ankara, Turkey

G. Eke · N. Hasirci · V. Hasirci (✉)  
BIOMATEN, METU Center of Excellence in Biomaterials and  
Tissue Engineering, Biotechnology Research Unit Bldg,  
06800 Ankara, Turkey  
e-mail: vhasirci@metu.edu.tr

G. Eke  
Department of Chemistry, Faculty of Arts and Sciences, Ahi  
Evran University, 40100 Kirsehir, Turkey

A. M. Kuzmina · E. I. Shishatskaya  
Siberian Federal University, Svobodnyi Avenue,  
Krasnoyarsk 660041, Russia

A. V. Goreva · E. I. Shishatskaya  
Institute of Biophysics SB RAS, Akademgorodok,  
Krasnoyarsk 66003, Russia

N. Hasirci · V. Hasirci  
Department of Biotechnology, Middle East Technical  
University, 06800 Ankara, Turkey

N. Hasirci · V. Hasirci  
Department of Biomedical Engineering, Middle East Technical  
University, 06800 Ankara, Turkey

N. Hasirci  
Department of Chemistry, Middle East Technical University,  
06800 Ankara, Turkey

V. Hasirci  
Department of Biological Sciences, Middle East Technical  
University, 06800 Ankara, Turkey

relatively low side effects, maximum drug availability at the target site, and avoidance of the systemic circulation. Many bioactive agents, however, do not have the necessary physicochemical properties for satisfactory efficacy when applied topically [1]. Transdermal skin treatment requires the absorption of drug through the skin into the body. One of the biggest challenges in developing an effective system is the transfer of the drug through the tightly structured stratum corneum when the skin is not compromised [2]. There are three layers of skin that needs to be crossed and each has a different role. The epidermis is the outer layer and serves as a barrier against the environment and stratum corneum is the outermost layer of the epidermis [3]. The dermis gives the skin its mechanical strength. The deepest layer in the subcutis or the subcutaneous layer which helps conserve the heat and act as a shock absorber. The hair follicles and sweat glands of the skin are believed to serve as the route of entry for nano sized drug carriers. Encapsulation of a drug in a carrier enables the drug to diffuse into the skin and be released in the deeper layers of the skin using the hair follicles and the sweat glands because the follicles extend deep into the skin [4, 5]. There is a rich capillary blood supply available in the subcutaneous layer to transport solutes like drugs that diffuse out of the follicle. As a result, there is substantial interest in targeted follicular delivery via nanoparticles loaded with drugs [6, 7].

Nanoparticles were developed as an important strategy to deliver conventional drugs like antibiotics [8], recombinant proteins [9], vaccines [10], nucleotides [11], and growth factors [12]. The special advantage of nanoparticles is their ability to reach tissues that larger controlled release carriers cannot and release their contents rather than being restricted to the circulation and releasing their content systemically. With the developments in nanotechnology and their introduction to the biomaterials field, various types of nano sized drug delivery systems such as nanocapsules and spheres, complexes, liposomes, dendrimers and emulsions were developed. The use of nano sized drug carriers constructed from biodegradable polymers are also increasingly used because even if they penetrate untargeted tissues they do not stay there long but disintegrate by time [12–14].

Polyhydroxyalkanoates (PHAs) are among the natural polymers preferred for the production of drug delivery vehicles, because they can be produced by in a range of compositions and properties, such as degradation rate [15, 16]. PHAs are linear, semicrystalline, thermoplastic and biocompatible polymers of microbiological origin which have a certain degree of biodegradability in the body [14, 17, 18]. Their biological origin is an advantage over the other major polyester group, the polylactides, which are petroleum based. The most abundantly studied PHAs are poly(3-hydroxybutyrate) and its copolymers with 3-hydroxyvalerate, poly(3-

hydroxybutyrate-co-3-hydroxyvalerate) (PHBV), with varying HV contents. PHBV has been used in controlled release systems (anticancer agents, pain relievers, antibiotics, growth factors), biodegradable bone plates, and in tissue engineering (cornea, bone, cartilage) [19, 20].

In this study, *in vitro* and *in vivo* transdermal permeation of PHBV micro/nanoparticles was studied by using Nile Red as a fluorescent agent to stain the polymer and help to follow transference of polymeric particles. The delivery systems studied were constructed using PHBV micro/nanospheres with different diameters, and this helped determine the importance of the size of the particles on the penetration was studied. The size distribution, morphology, cytotoxicity, uptake by cells and penetration of the skin were studied using these particles in addition to testing the skin reactions to the application of the particle.

## 2 Experimental

### 2.1 Materials

PHBV (HV content 11 %, M), thiazolyl blue tetrazolium bromide cell proliferation assay (MTT) kit, and Nile Red were purchased from Sigma-Aldrich (St. Louis, Missouri, USA). Polyvinyl alcohol (PVA, MW  $1.5 \times 10^4$ ) was purchased from Fluka (St. Louis, Missouri, USA). L929 cell line was obtained from the Foot-and-Mouth Disease Institute (Ankara, Turkey). Dulbecco's Modified Eagle Medium (DMEM), high glucose (with phenol red), fetal bovine serum (FBS), and laboratory grade penicillin/streptomycin (10,000 units/mL Penicillin, 10 mg/mL Streptomycin) were purchased from HyClone (Logan, Utah, USA).

### 2.2 Preparation of Nile red stained PHBV micro/nanospheres

Oil-in-water (o/w) method was used for the production of micro and nanospheres. Nile Red (0.1 mL, 0.01 % in acetone) was added into a solution of PHBV in dichloromethane (1.2 mL, 10 %, w/v). Then this was added into an aqueous solution of PVA (4 mL, 4 %, w/v) and sonicated for 15 s in an ice bath. This emulsion (o/w) was diluted with aqueous PVA solution (10 mL, 0.3 %, w/v), mixed with a magnetic stirrer overnight at room temperature for solvent (DCM) evaporation. The spheres were separated by centrifugation and lyophilized.

### 2.3 Preparation of micro/nanospheres with different sizes

In order to obtain PHBV particles with different sizes, different centrifugation rates and durations were applied.

To obtain the largest size microsphere fraction the suspension was centrifuged at 12,000 rpm (15,455 g) for 10 min. Medium and small sized nanospheres were obtained by centrifuging the oil in water suspension at 13,500 rpm (18,138 g) for 10 min and at 14,500 rpm (22,566 g) for 40 min, respectively.

## 2.4 Characterization

### 2.4.1 Examination of the spheres with scanning electron microscopy

An aqueous suspension of PHBV nanoparticles (100  $\mu$ L, 1.2 %) was added onto carbon tapes (Electron Microscopy Sciences, USA) attached to SEM stubs, dried at room temperature and then Au–Pd sputter coated (2 nm) under vacuum before examining with QUANTA 400F field emission SEM (Netherlands). The SEM images were used to study the morphology of the spheres of the particles as well as to measure the dimensions and calculate the average sizes of the particles with Image J software (NIH).

### 2.4.2 Particle size distribution analysis

The size distribution of the micrometer sized PHBV particles was determined by Mastersizer (Malvern Instruments 2000, UK) and the nanometer sized PHBV particles were studied with a Malvern Nano ZS90 system (UK).

## 2.5 In vitro studies

### 2.5.1 L929 mouse fibroblast cell culture

L929 cells were cultured in (DMEM, high glucose) supplemented with 10 % FBS and 1 % penicillin/streptomycin (100 unit). They were maintained in an incubator with 5 % CO<sub>2</sub> at 37 °C (Sanyo MCO-17AIC, Japan) until confluency. Before seeding, the cells were detached from the flask by treatment with trypsin–EDTA solution (3 mL, 0.05 % in PBS) for 5 min. Then culture medium (6 mL) was added to stop trypsin activity. The cell suspension was centrifuged (3,000 rpm, 5 min) and the cell pellet was resuspended in the medium (2 mL). The cells were counted with a hemocytometer (Blau Brand, Germany), seeded onto 24 well and 6 well tissue culture plates for proliferation and uptake studies, respectively.

### 2.5.2 Determination of cell numbers with MTT assay

Nile Red loaded micro/nanospheres (0.5 and 1 mg/mL) were suspended in the culture medium and added into 24-well plates. L929 cells (20,000) were seeded in the wells and incubated (37 °C, 5 % CO<sub>2</sub>) for 24 h. Then, the

medium was removed, wells were washed twice with sterile PBS, MTT solution (1 mL) was added into each and incubated for 3 h at 37 °C in a CO<sub>2</sub> incubator. The MTT solution was replaced with acidified isopropanol (1 mL) and formazan crystals formed were dissolved. Aliquots of formazan solution (200  $\mu$ L) were put in a 96-well plate in triplicates and absorbances were measured at 550 nm using a UV spectrophotometer (Thermo Scientific Multiscan Spectrum, Type 1500, USA). This was repeated on days 3 and 7. All the experiments were conducted in triplicate and cell-free medium was used as the blank. The OD values were converted to number of cells by a calibration curve.

### 2.5.3 Micro/nanosphere uptake by L929 cells

Interaction of micro and nanospheres with the cells were studied with L929 cells. After 24 h of incubation in DMEM, high glucose medium supplemented with 10 % FBS and 1 % penicillin/streptomycin (100 unit), L929 cells (10,000) were seeded into a 6-well plate containing Nile Red stained spheres (0.2 mg/mL) in growth medium. After 24 h of incubation, cells were fixed with paraformaldehyde (4 %, 1 mL), stained with 4',6-diamidino-2-phenylindole and FITC-conjugated phalloidin for the nucleus and the cytoskeleton, respectively [21]. After staining, the particles and the cells were observed with confocal laser scanning microscopy (CLSM) (Leica DM2500, Germany) at room temperature.

## 2.6 In vivo studies

### 2.6.1 Animal model

Experiments were conducted on male, 14 week old, BALB/c mice, 20–25 g each. They were kept under standard environmental conditions in an animal house in cages, two animals per cage, fed a standard laboratory diet and water in accordance with SS R ISO 10993-10-2009 (State Standard of Russian Federation, elaborated based ISO), for the investigation of skin irritation, as approved by the Institutional Animal Ethical Committee on Biomedical Ethics of Siberian Federal University (Russia).

### 2.6.2 Treatment of mice and application of polymeric particles

Dorsal sections of the mice were shaved 1 day before application of the PVA solution (8 %, carrying 5 mg PHBV in 5 mL) was prepared. After removal of the hair, skin was swabbed with pure ethanol to sterilize to dry the skin [22] and then with the particle suspension (1 mL) with a 2 min massage. Controls were treated exactly the same way only without the application of the formulation.

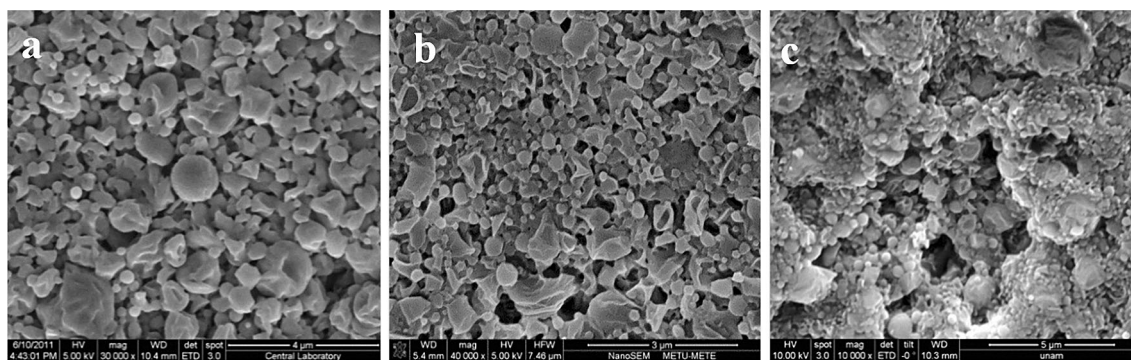


**Fig. 1** SEM micrographs of PHBV particles fractionated with centrifugation using different duration and velocity: **a** 10 min at 12,000 rpm (Bar 4  $\mu\text{m}$ ), **b** 10 min at 13,500 rpm (Bar 3  $\mu\text{m}$ ), **c** 40 min at 14,500 rpm (Bar 5  $\mu\text{m}$ )

After 4, 24 h, 3, 5 and 10 days, the animals were sacrificed with an overdose of ether. Skin samples (approximately  $1 \times 1 \text{ cm}^2$ ) were removed and used in histology after staining with Hematoxylin-Eosin, using light microscopy (Leica DM6000B, Germany). For the determination of the PHBV, gas chromatography-mass spectrometry (GC–MS) (GCD Plus, Hewlett Packard, USA) equipped with a  $30 \text{ m} \times 0.25 \text{ mm}$  HP-5 (polysiloxane, 5 % diphenyl and 95 % dimethyl) fused silica capillary column were used. For each dose and sample 2 animals were used.

### 2.6.3 Determination of the polymer of the micro/nanospheres in the skin with GC–MS

The skin samples were dried at  $60^\circ\text{C}$  overnight and approximately 10 mg was used to determine the amount of polymer in the skin using the GC–MS.

The skin sample was refluxed in chloroform: methanol: sulfuric acid (1:0.85:0.15) for 140 min at  $100^\circ\text{C}$  in a thermostatically regulated bath. After the digestion, distilled water (0.5 mL) was added and the tube was shaken for 1 min. After phase separation, the organic phase was transferred into a vial and analyzed using a GC–MS.

### 2.6.4 Histology

The tissue samples were fixed in 10 % formalin and embedded in paraffin. Sections (5  $\mu\text{m}$ ) were obtained using microtome and stained with hematoxylin and eosin then examined under a light microscope (Leica DM6000B, Germany). The general tissue reactions to micro and nanospheres were investigated.

## 2.7 Statistical analysis

All in vitro experiments were carried out in triplicates and the in vivo in duplicates. Significant differences in control and test groups were determined using Mann–Whitney *U* test. The

**Table 1** Size and polydispersity indices of PHBV micro and nanospheres ( $n = 2$ )

Property	Sample		
	Submicro	Nano	Low Nano
Mean diameter (nm)	$1900 \pm 157$	$426 \pm 74$	$166 \pm 22$
PI	$0.8 \pm 0.1$	$0.3 \pm 0.1$	$0.1 \pm 0.0$
Size range (nm)	400–12,000	190–712	80–542

differences were considered as statistically significant for the *P* values smaller than 0.05.

## 3 Results and discussion

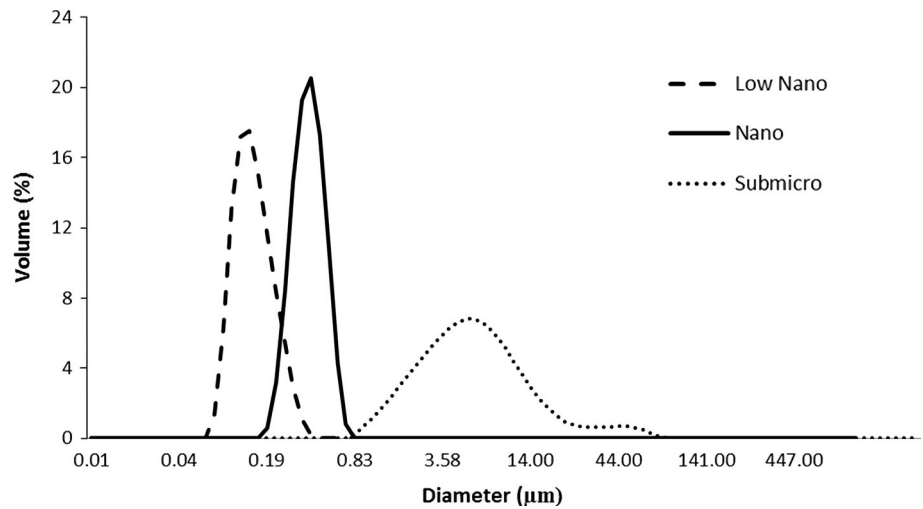
### 3.1 Micro/nanosphere characterization

Production of PHBV particles was carried out with 10 % (w/v) polymer solution in dichloromethane. This concentration was chosen based on previous studies with similar polymers [12, 23]. SEM micrographs show round, spherical particles with smooth surfaces (Fig. 1).

Three micro/nanosphere populations with different sizes were obtained. The calculations based on measurements on SEM micrographs showed that by changing the time and speed of centrifugation, it was possible to fractionate the particles into bathes with different sizes (Table 1; Fig. 1). The largest (1.9  $\mu\text{m}$ ) particles were obtained with the lowest *g* value and the smallest particles (166 nm) with the highest *g* value (Fig. 1a, b, c). It was reported that the particle size could be controlled by changing the preparation parameters, such as the sonication time and frequency [24], surfactant concentration, polymer concentration and centrifugation speed, [12, 25, 26].

In this study the change of size was not affected by the preparation conditions but by separation conditions. PI of these submicro, nano and low nano particles were found to be

**Fig. 2** Particle size distribution of PHBV particles. **a** low nano, **b** nano, **c** submicro



0.8, 0.3 and 0.1, respectively, indicating that the smallest fraction had the most narrow particle size distribution as also was confirmed by the sharpness of the peak in Fig. 2a and the size range in Table 1. This is also expected because the lowest diameter particles were obtained after three successive centrifugations and as the number of centrifugations increased the PI value was also decreased because removal of larger particles at earlier centrifugations leaves behind narrower distributions. This is supported by the studies in the literature, too [27, 28]. The sizes obtained were suitable for use in the in vitro and in vivo tests.

### 3.2 In vitro tests

#### 3.2.1 Influence of particle size and concentration on cell proliferation

Different sized PHBV micro/nanospheres were tested for their effect on cell proliferation using L929 mouse fibroblasts and the MTT test (Fig. 3). Cell proliferation studies using high or low dose of particles are presented in Fig. 3. In both doses the control showed the highest and the micrometer sized nanoparticles showed the lowest proliferation. In Fig. 3a, no significant effect of particle size on proliferation was observed. The effect of particles on cell proliferation was significant when the particle concentration was higher (Fig. 3b).

When the concentration of the particles was low (0.5 mg/mL), the proliferation rates of the L929 cells for all particle sizes at each time point (Fig. 3a) were found to be statistically significant according to Mann–Whitney *U* test ( $P < 0.05$ ).

When the concentration was increased to 1 mg/mL, L929 cell proliferation rate decreased for all sample types over the whole duration of the test (Fig. 3b). For nano and submicro sized particles the proliferation rates increased in

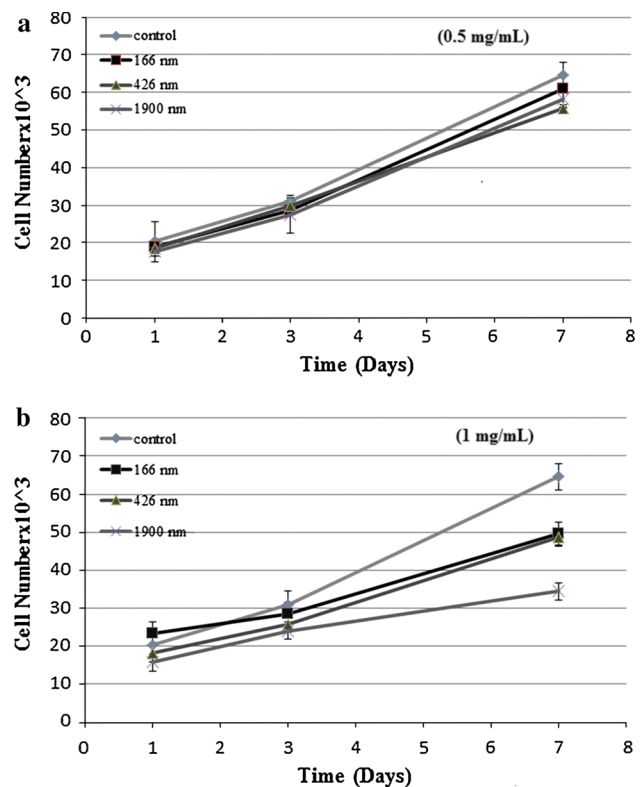


**Fig. 3** Effect of particle size and concentration of micro/nanospheres on L929 proliferation ( $n = 3$ ). **a** LOW dose (0.5 mg/mL), **b** high dose (1 mg/mL)

a statistically significant manner throughout the whole duration of the test. For the low nano sized particles, however, no statistically significant difference could be observed between days 1 and 3.

These cells did not show a change in their shape implying that the decrease is not due to a negative effect like toxicity which could have been observed by light microscopy.

**Fig. 4** Confocal and Transmission micrographs of nano (166 nm) sized, Nile Red stained PHBV spheres in contact with L929 cells for 24 h ( $\times 160$ ). **a** Cytoskeleton (green, stained with Phalloidin-FITC), **b** nanoparticles (stained with Nile Red), **c** overlay of **(a)** and **(b)**, **d** transmission image of the cell

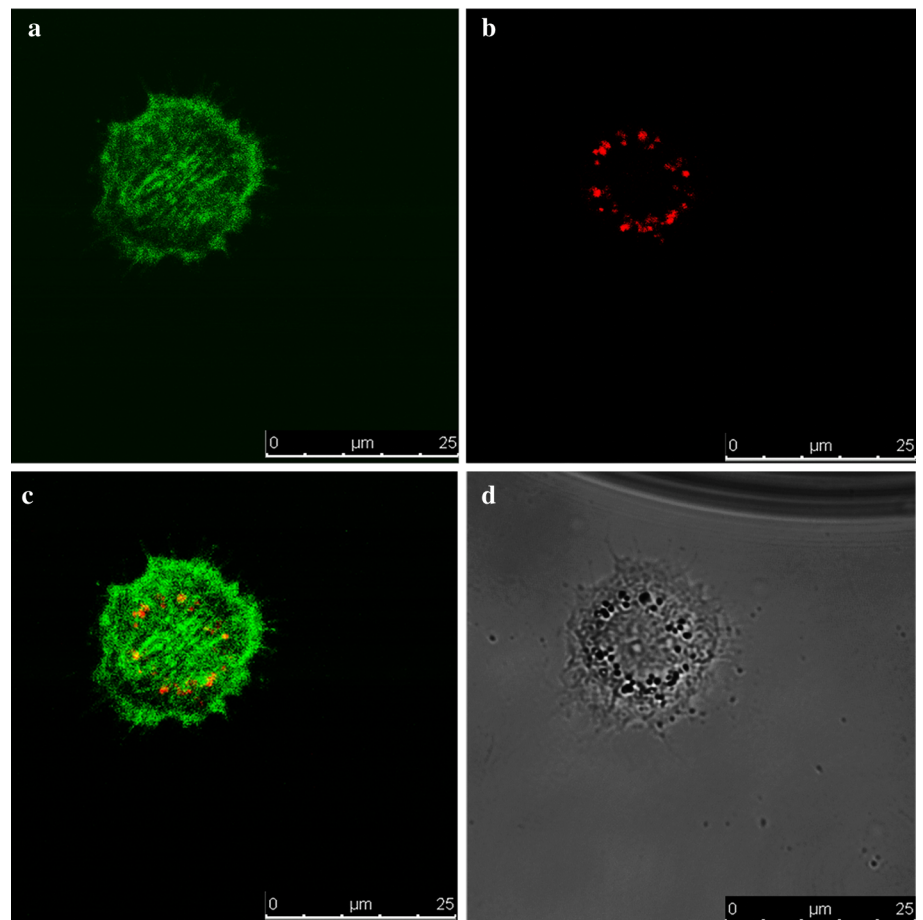


**Fig. 5** Confocal and Transmission micrographs (426 nm) sized, Nile Red stained PHBV spheres in contact with L929 cells for 24 h ( $\times 40$ ). **a** Cytoskeleton (green, stained with Phalloidin-FITC), **b** nanoparticles (stained with Nile Red), **c** overlay of **(a)** and **(b)**, **d** transmission image of the cell

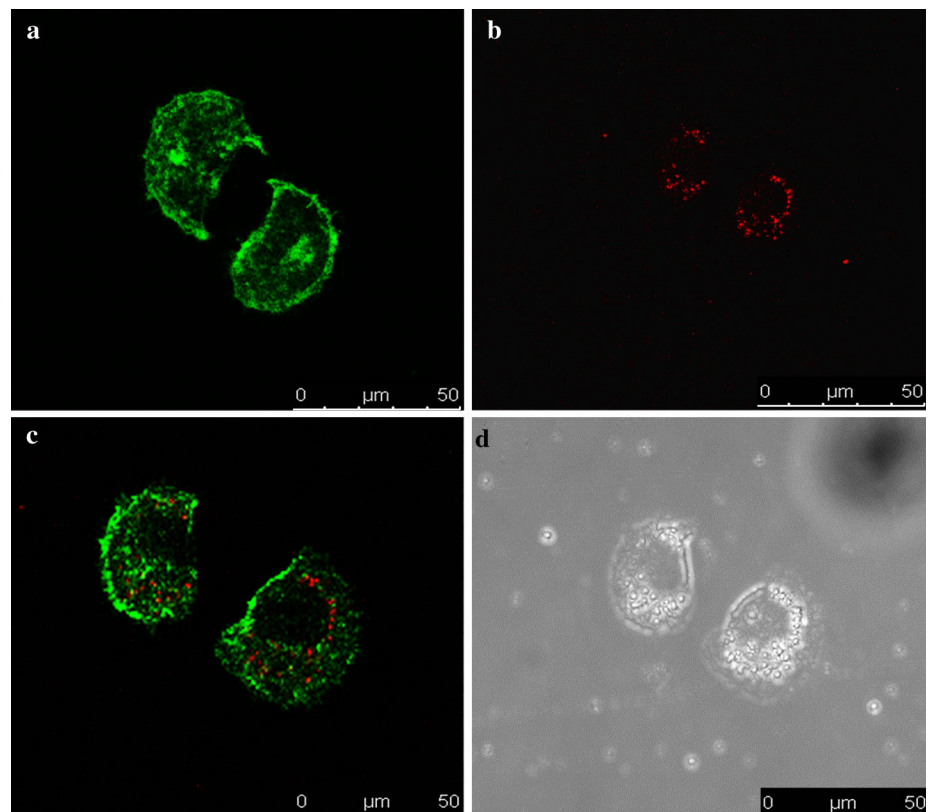


**Fig. 6** Confocal and Transmission micrographs of submicron (1.9  $\mu\text{m}$ ) sized, Nile Red stained PHBV spheres in contact with L929 cells for 24 h ( $\times 40$ ). **a** Cytoskeleton (green, stained with Phalloidin-FITC), **b** nanoparticles (stained with Nile Red), **c** overlay of (a) and (b), **d** transmission image of the cell

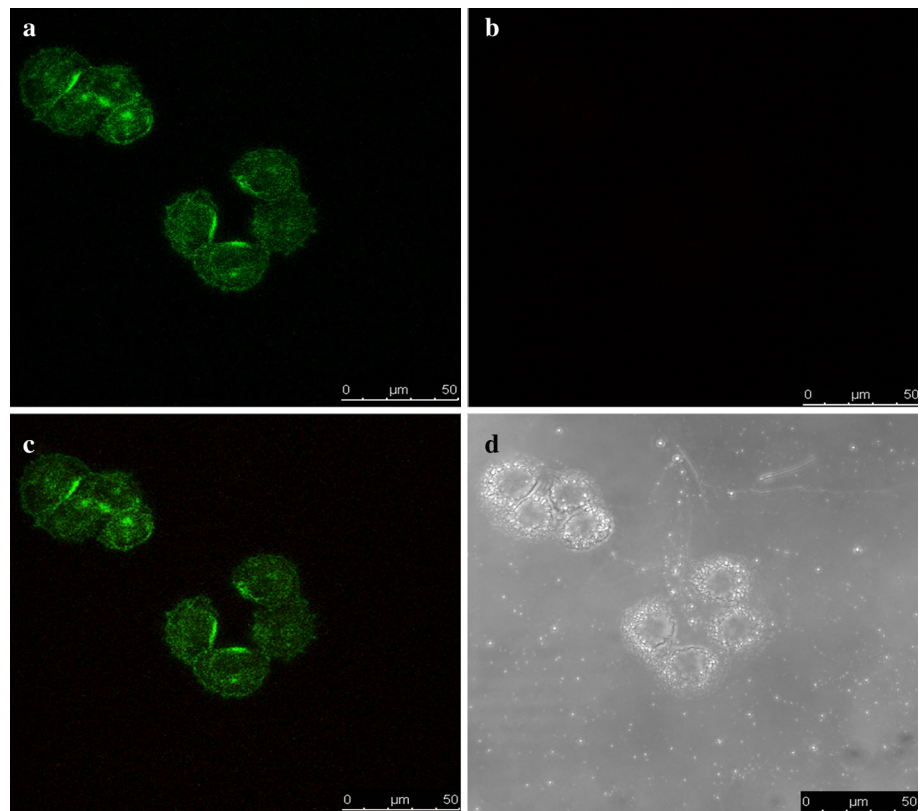


**Table 2** Penetration of PHBV micro/nanospheres into mouse skin (Applications: 5 mg total, 1 mg/mL) ( $n = 2$ )

Average particle diameter	Polymer penetration (percent of input) and Time				
	4 h	24 h	3 days	5 days	10 days
1.9 $\mu\text{m}$	1.0	0.9	0.4	0.2	0.1
426 nm	1.3	–	0.6	0.5	0.1
166 nm	0.6	0.3	0.9	0.6	–

It is stated that particles with a size up to about 100–200 nm can be internalized by receptor-mediated endocytosis, while larger particles have to be taken up by phagocytosis [13, 24]. It is also reported that the larger particles (greater than 1  $\mu\text{m}$ ) are taken up by a mechanism other than endocytosis, such as fluid-phase pericytosis [13, 24]. It is expected that the small size particles could improve efficacy of the particle based topical drug delivery systems because of more availability within the cell.

About the effect of particulate matter’s concentration Sohaebuddin et al. [29] in their study on 3T3 and RAW cells observed suppression of cell proliferation when higher particle concentrations are used and explained this by the dispersion and agglomeration of these particles. It was found by Errico et al. [26] that PHB based nanoparticles were safe and exhibited high cell proliferation

when used in low doses and their sizes were in the range 55–100 nm. They also observed that this suppression was dependent on the cell type. These findings support the results presented in Fig. 3 of this study.

In the literature, however, the issue of size and proliferation is somewhat more complicated.

Wang et al. [30] reported that, cells incubated with polymeric nanospheres had a better growth than with microspheres but they also stated that microspheres were hardly phagocytized due to their large size. They also observed that when the polymer contained higher proportions of PEG phagocytosis decreased and viability increased. These findings indicate that penetration into cells could be both better and worse for proliferation, and therefore, it is controversial. In the present study the largest size particles (1,900 nm) led to a higher suppression of cell proliferation than with smaller particles (Fig. 3b).

### 3.2.2 Penetration of micro/nanospheres into L929 cells

Initial studies of particle penetration into the cells were carried out with the three batches of particles with different sizes. Figures 4 and 5 show that the cells take up the low and mid nano sized particles. An interesting finding was that the nanospheres were generally located in the cytoplasm near the nuclei. The larger (submicro) particles,

**Fig. 7** Histology of the skin samples from BALB/c mice without treatment with micro/nanoparticles. (Rectangle)-epidermis, (right arrow)-pilosebaceous, (square braces)/hb-hair bars. The bar is 900  $\mu\text{m}$

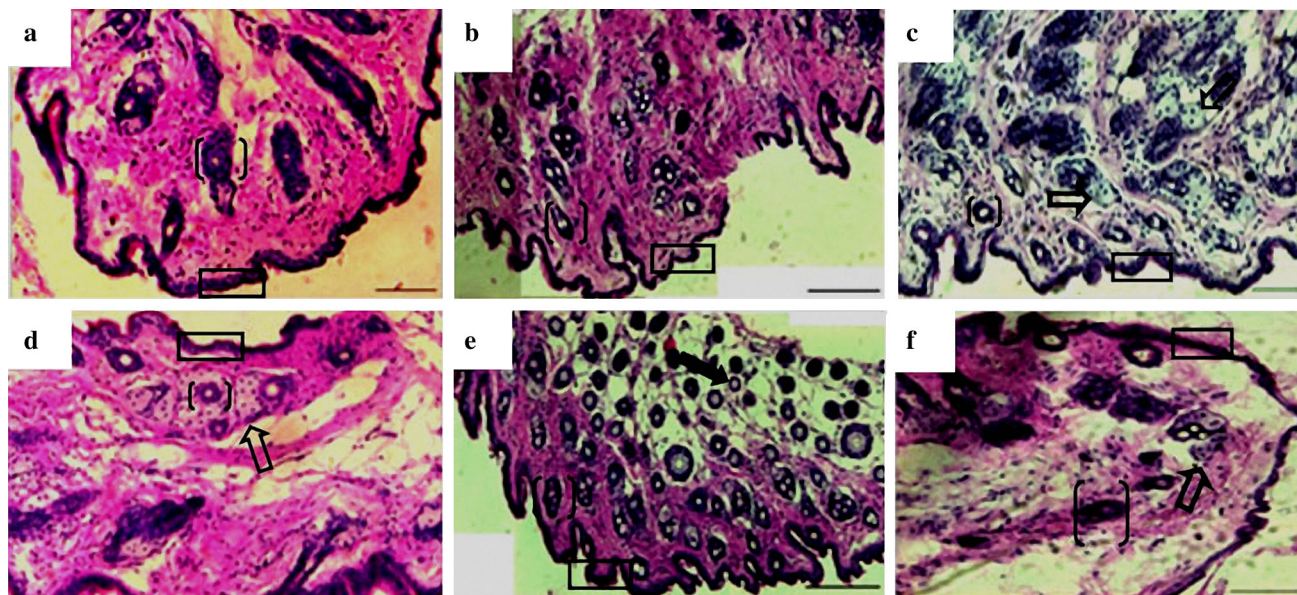
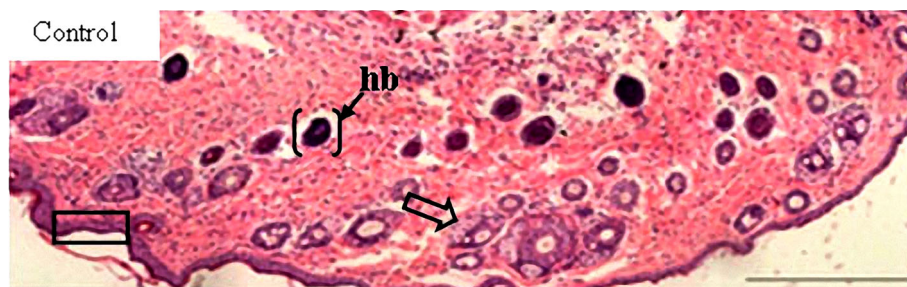


**Fig. 8** Histology of the skin samples from BALB/c mice after treatment with micro/nanoparticles in PVA (8 %) suspension for 10 days. **a** 166 nm/4 h, **b** 426 nm/4 h, **c** 1.9  $\mu\text{m}$ /4 h, **d** 166 nm/24 h, **e** 426 nm/24 h, **f** 1.9  $\mu\text{m}$ /24 h. (Rectangle) epidermis, (right arrow) pilosebaceous, (filled right arrow) pilosebaceous reaching a

hypodermic-fatty layer, (square braces)/hb-hair bars, si-slight infiltration. The bar is 900  $\mu\text{m}$ . It is seen that epidermis is of ordinary thickness, pilosebaceous units are fully formed reaching a hypodermic-fatty layer. Follicles are seen to contain hair bars. Slight lymphohistiocytic infiltration is observed perifollicularly

however, seemed to be unable to penetrate into the cells (Fig. 6).

Desai et al. [31] reported intracellular uptake of nanoparticles and showed that this depends on the size and hydrophobicity. In their study the uptake decreased with increasing size and hydrophilicity and they stated that it is difficult to internalize the submicron sized particles. This supports the observation about the inability of the 1.9  $\mu\text{m}$  diameter particles to penetrate inside the cells. Distinction has to be made in terms of the mode of intracellular uptake. Intracellular uptake of particulates is proposed to be either by phagocytosis or by endocytosis [32]. It was reported that nanoparticles around 500 nm are taken up by macrophages by phagocytosis [33]. However, for the smaller nanoparticles, the main route of cellular entry is through fluid phase endocytosis and it leads to entrapment inside intracellular vehicles, such as endosomes or lysosomes [34]. In the present case the ca. 500 nm particles

could be observed outside the nuclear membrane as distinct groups of particulates. Furthermore, they appeared to be intact, otherwise, lysis by lysosomal enzymes would release the Nile Red into the medium causing it to stain all the organelles with lipid components.

### 3.3 In vivo tests

#### 3.3.1 Penetration of micro/nanospheres into mouse skin

Transdermal delivery systems are being increasingly used in the clinic for delivery of small, lipophilic drugs for low doses [35, 36]. The question being addressed in this study was whether the penetration depth in healthy skin differs with size of the particles. Therefore, the penetration of Nile Red stained PHBV micro/nanospheres were studied on mouse skin in the presence of a penetration enhancer

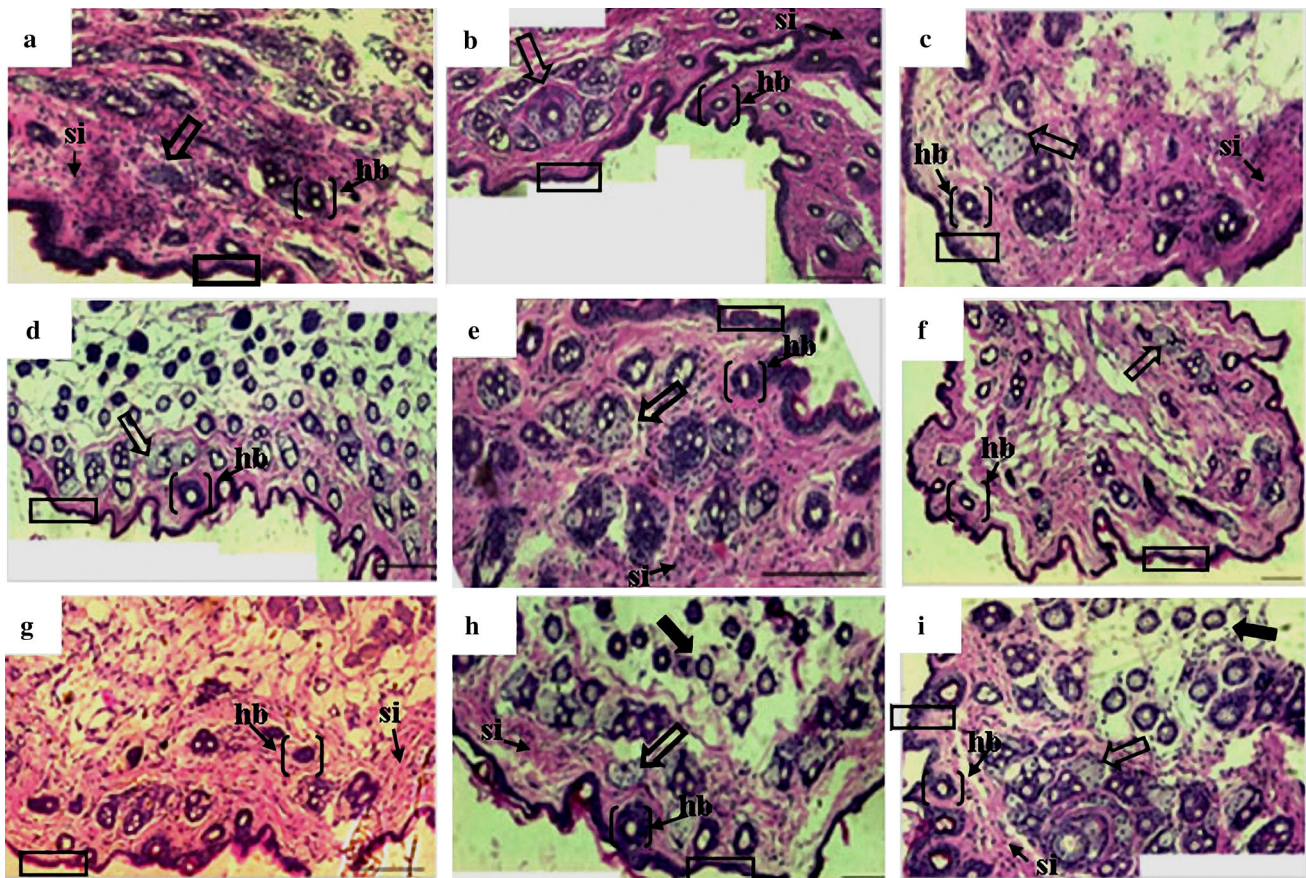


**Fig. 9** Histology of the skin samples from BALB/c mice without treatment with micro/nanoparticles in PVA (8 %) suspension for 10 days. **a** 166 nm/3 day, **b** 426 nm/3 day, **c** 1.9  $\mu$ m/3 day, **d** 166 nm/5 day, **e** 426 nm/5 day, **f** 1.9  $\mu$ m/5 day, **g** 166 nm/

10 day, **h** 426 nm/10 day, **i** 1.9  $\mu$ m/10 day. (rectangle)-epidermis, (right arrow)-pilosebaceous, (filled right arrow)-pilosebaceous reaching a hypodermic-fatty layer, (square braces)/hb-hair bars, si-slight infiltration. The bar is 900  $\mu$ m

(PVA). PHBV was suspended in PVA (8 %) and applied onto the skin of the mice.

Upon sacrifice, patches of skin were removed, treated as stated above, the skin was analyzed with histology and the amount of polymer coming from micro/nanospheres penetrated in the skin was determined using GC-MS spectroscopy. It is apparent that particles penetrated into the skin at comparable levels (Table 2). Soon after application, about 1 % was found in the skin and this gradually decreased by tenfold in 10 days. This shows that PHBV nanoparticles or the polymer that might result from its degradation can penetrate the stratum corneum to a small extent. According to the literature particles lower than 100 nm in diameter penetrate the skin while the particles with sizes above 200 nm do not [7, 37, 38]. Thus, our results either contradict this or small sized particles (lower than 200 nm) in each sample penetrated the skin. In either case this approach could be sufficient to deliver skin therapeutics by transdermal applications, using nanoparticles especially if the dose of the active agent is high enough.

### 3.3.2 Histopathological analysis of mouse skin

The depth of penetration of three different sized PHBV micro/nanosphere samples in mouse skin was investigated by topical application to BALB/c mice.

Histological examination of the skin of mice from the 3 test and 1 control group showed an identical morphology of the skin. No signs of necrosis or festering inflammation were observed in any group. Epidermis was of ordinary thickness (Figs. 7, 8, 9), pilosebaceous units were fully formed (Figs. 8a, c, d, f; 9a–f, h, i), reaching a hypodermic-fatty layer (Figs. 8e; 9h, i). Follicles contained hair bars (Figs. 7, 8, 9). Slight lymphohistiocytic infiltration was recorded perifollicularly (Figs. 8, 9).

In none of the skin sections the presence of the particles could be detected, which probably can be explained by the size of the particles being lower than the resolution of the light microscopic examination. This is highly probable because unfixed skin sections when tested for polymer presence using GC-MS showed the polymer (weighing about

100 µg) was in the skin indicating that the particles penetrated the skin but could not be visualized. The absence of particles in the upper layers of the epidermis and on the skin surface could also be explained by the use of nonpolar solvents in the fixing procedure which could have led to the dissolution of the particles, and therefore, decreased the ability to detect them.

#### 4 Conclusion

The aim of transdermal delivery systems is to deliver low molecular weight agents safely and effectively without irritating the stratum corneum or the deeper tissue layers. Polymeric particles are promising carriers for use in these delivery applications. They can be made in various sizes, from various materials, can carry molecules of different chemistries and be modified for targeting purposes. Depending on their properties, polymeric particles may persist in vivo for different periods. PHAs, known as slow degrading biopolymers, could be used as carriers in the design of drug delivery systems in such treatments as that of oncological processes. As such, they are indispensable drug carriers. These results give us ground to consider the use of bacterial PHBV in the development of systems for transdermal transport. Particles smaller than 450 nm, as obtained in this study, appear to be promising therapeutic tools for the treatment of compromised skin.

**Acknowledgments** The study was supported by the Government of the Russian Federation (Decree No. 220 of 09.04.2010) (Agreement No. 11.G34.31.0013) and (Grant № MD-3112.2012.4). We gratefully acknowledge the EC FP7 SKINTREAT project and the State Planning Organization (Turkey) for the grant to establish BIOMATEN. Mr. A. Büyüksungur is acknowledged for his contributions with CLSM.

#### References

- Sloan KB, Wasdo SC, Rautio J. Design for optimized topical delivery: prodrugs and a paradigm change. *Pharm Res.* 2006;26:2729–47.
- Yow HN, Wu X, Routh AF, Guy RH. Dye diffusion from microcapsules with different shell thickness into mammalian skin. *Eur J Pharm Biopharm.* 2009;72:62–8.
- Gawkroder DJ. *Dermatology*, vol. 1. New York: Edinburgh Churchill Livingstone Inc; 2002.
- Prausnitz MR, Langer R. Transdermal drug delivery. *Nature Biotechnol.* 2008;26:1261–8.
- Arora A, Prausnitz MR, Mitragotri S. Micro-scale devices for transdermal drug delivery. *Int J Pharm.* 2008;364:227–36.
- Wosicka H, Cal K. Targeting to the hair follicles: current status and potential. *J Dermatol Sci.* 2010;57:83–9.
- Prow TW, Grice JE, Lin LL, Faye R, Butler M, Wurme EMT, et al. Nanoparticles and microparticles for skin drug delivery. *Adv Drug Deliv Rev.* 2011;63:470–91.
- Gursel I, Korkusuz F, Türesin F, Alaeddinoğlu NG, Hasirci V. In vivo application of biodegradable controlled antibiotic release systems for the treatment of implant-related osteomyelitis. *Biomaterials.* 2001;22:73–80.
- Jahanshahi M, Babaei Z. Protein nanoparticle: a unique system as drug delivery vehicles. *Afr J Biotechnol.* 2008;7:4926–34.
- Rieux AD, Fievez V, Garinot M, Schneider YJ, Pr at V. Nanoparticles as potential oral delivery systems of proteins and vaccines: a mechanistic approach. *J Control Release.* 2006;116:1–27.
- Xia T, Kovochich M, Liong M, Meng H, Kabehie S, George S, et al. Polyethyleneimine coating enhances the cellular uptake of mesoporous silica nanoparticles and allows safe delivery of siRNA and DNA constructs. *ACS Nano.* 2009;3:3273–328.
- Yilgor P, Hasirci N, Hasirci V. Sequential BMP-2/BMP-7 delivery from polyester nanocapsules. *J Biomed Mater Res Part A.* 2010;93:528–36.
- Yin WK, Feng SS. Effects of particle size and surface coating on cellular uptake of polymeric nanoparticles for oral delivery of anticancer drugs. *Biomaterials.* 2005;26:2713–22.
- Hasirci V, Vrana E, Zorlutuna P, Ndreu A, Yilgor P, Basmanav FB, et al. Nanobiomaterials: a review of the existing science and technology, and new approaches. *J Biomater Sci Polym Edn.* 2006;17:1241–68.
- Hasirci V, Yucel D. Polymers used in tissue engineering. *Encyclopedia Biomater Biomed Eng.* 2007;1:1–17.
- Boyandin AN, Prudnikova SV, Filipenko ML, Khrapov EA, Vasil'ev AD, Volova TG. Biodegradation of polyhydroxyalkanoates by soil microbial communities of different structures and detection of PHA degrading microorganisms. *Appl Biochem Microbiol.* 2012;48:28–36.
- Sudesh K, Abe H, Doi Y. Synthesis, structure and properties of polyhydroxyalkanoates: biological polyesters. *Prog Polym Sci.* 2000;25:1503–55.
- Shishatskaya E, Goreva A, Kalacheva G, Volova TG. Biocompatibility and resorption of intravenously administered polymer microparticles in tissues of internal organs of laboratory animals. *J Biomater Sci Polym Edn.* 2011;22:2185–203.
- Hasirci V, Yilgor P, Endogan T, Eke G, Hasirci N. Polymer fundamentals: Polymer synthesis. In: Ducheyne P, Healy K, Hutmacher D, Grainger DW, Kirkpatrick CJ editors. *Comprehensive Biomaterials* 2011;1:349–371.
- Goreva AV, Shishatskaya EI, Volova TG, Sinskey AJ. Characterization of polymeric microparticles based on resorbable polyesters of oxyalkanoic acids as a platform for deposition and delivery of drugs. *Polym Sci Series A Med Polym.* 2012;54:94–105.
- Davidson PM, Ozcelik H, Hasirci V, Reiter G, Anselme K. Microstructured surfaces cause severe but non-detrimental deformation of the cell nucleus. *Adv Mater.* 2009;21:3586–90.
- Goope NV, Roberts DW, Webb P, Cozart CR, Siitonen PH, Latendrese JR, et al. Quantitative determination of skin penetration of PEG-coated Cd Se quantum dots in dermabrased but not intact SKH-1 hairless mouse skin. *Toxicol Sci.* 2009;1:37–48.
- Chen WH, Tang BL, Tong YW. PHBV Microspheres as tissue engineering scaffold for neurons. *IFMBE Proc.* 2009;23:1208–12.
- Xiong YC, Yao YC, Zhan XY, Chen GQ. Application of polyhydroxyalkanoates nanoparticles as intracellular sustained drug-release vectors. *J Biomater Sci.* 2010;21:127–40.
- Crowley TJ, Meadows ES, Kostoulas E, Doyle FJ. Control of particle size distribution described by a population balance model of semi batch emulsion polymerization. *J Process Control.* 2000;10:419–32.
- Errico C, Bartoli C, Chiellini F, Chiellini E. Poly(hydroxyalkanoates) based polymeric nano particles for drug delivery. *J Biomed Biotechnol.* 2009;10:1–10.
- Abulatefeh SR, Sebastian G, Spain SG, Thurecht KJ, Aylott JW, Chan WC, Garnetta MC, Cameron Alexander C. Enhanced uptake of nanoparticle drug carriers via a thermoresponsive shell

- enhances cytotoxicity in a cancer cell line. *Biomater Sci.* 2013;1:434–42.
28. Simone Lerch S, Dass M, Musyanovych A, Landfester K, Mailander V. Polymeric nanoparticles of different sizes overcome the cell membrane barrier. *Eur J Pharm Biopharm.* 2013;84:265–74.
  29. Sohaebuddin SK, Thevenot PT, Baker D, Eaton JW, Tang L. Nanomaterial cytotoxicity is composition, size, and cell type dependent. *Particle Fibre Toxicol.* 2010;7:22–30.
  30. Wang W, Zhou S, Guo L, Zhi W, Li X, Weng J. Investigation of endocytosis and cytotoxicity of poly-d, l-lactide-poly(ethylene glycol) micro/nano-particles in osteoblast cells. *Int J Nanomed.* 2010;5:557–66.
  31. Desai MP, Labhasetwar V, Walter E, Levy RJ, Amidon GL. The mechanism of uptake of biodegradable microparticles in Caco-2 cells is size dependent. *Pharm Res.* 1997;14:1568–73.
  32. Sahoo SK, Panyam J, Prabha S, Labhasetwar L. Residual poly-vinyl alcohol associated with poly (D, L-lactide-co-glycolide) nanoparticles affects their physical properties and cellular uptake. *J Controlled Release.* 2002;82:105–14.
  33. Foster KA, Yazdanian M, Audus KL. Microparticulate uptake mechanisms of in vitro cell culture models of the respiratory epithelium. *J Pharm Pharmacol.* 2001;53:57–66.
  34. Benfer M, Kissel T. Cellular uptake mechanism and knockdown activity of siRNA-loaded biodegradable DEAPA-PVA-g-PLGA nanoparticles. *Eur J Pharm Biopharm.* 2012;80:247–56.
  35. Wermeling DP, Banks SP, Hudson DA, Gill HS, Gupta J, Prausnitz MR. Micro needles permit transdermal delivery of a skin-impermeant medication to humans. *Proc Natl Acad Sci.* 2008;105:2058–63.
  36. Baroli B. Penetration of nanoparticles and nanomaterials in the skin: fiction or reality. *J Pharm Sci.* 2010;99:21–50.
  37. Tomoda K, Terashima H, Suzuki K, Inagi T, Terada H, Makino K. Enhanced transdermal delivery of indomethacin-loaded PLGA nanoparticles by iontophoresis. *Colloids Surf B.* 2011;88:706–10.
  38. Webster TJ. Editor. *Nanostructure science and technology: Safety of nanoparticles from manufacturing to medical applications.* Springer Science and Business Media, LLC. 2009 Available from URL: <http://www.springer.com/series/6331>. Accessed 15 Feb 2013.